Numerical modeling and testing of mechanical behavior of AM Titanium alloy bracket for aerospace applications

Available online at www.sciencedirect.com

ScienceDirect

Procedia Structural Integrity 5 (2017) 753–760

Structural Integrity Procedia

www.elsevier.com/locate/procedia

2nd International Conference on Structural Integrity, ICSI 2017, 4-7 September 2017, Funchal, Madeira, Portugal

Numerical modeling and testing of mechanical behavior of AM Titanium alloy bracket for aerospace applications

Eugenio Brusa, Raffaella Sesana*, Enrico Ossola

DIMEAS, Politecnico di Torino, Corso Duca degli Abruzzi 24, 10129 Torino, Italy

Abstract

A key issue in designing a new product made through the Additive Manufacturing (AM) is the prediction of mechanical properties of material. Several experimental results show that AM-based products are often affected by widespread porosity, low density regions within their volume and anisotropy. Those effects are due to the manufacturing process, despite of efforts spent to improve the process parameters. This paper presents the numerical modelling of a geometrically complex structural bracket for aerospace application, which was re-designed through a topological optimization and produced in Ti-6Al-4V by means of the AM. The design activity herein described required to resort to a suitable model of constitutive properties of material by facing the problem of a large number of porosity/low density areas, as detected by a tomographic analysis of the mechanical component. According to some references an equivalent isotropic and homogeneous model of material was applied. Nevertheless the limitations of that approach were investigated through a validation of the numerical model and a testing activity. It was demonstrated that the Finite Element model based upon the assumptions of homogeneous and isotropic material might be effective in predicting the material and component strength, at least in static design, but even in case of design against fatigue, provided that a suitable experimental characterization of material was performed. The procedure of optimization was then assessed and compared to some preliminary tests performed on the real component, thus providing a preliminary good practice to the industrial partner involved in this research activity.

Peer-review under responsibility of the Scientific Committee of ICSI 2017

* Corresponding author. Tel.: +39-011-0906907; fax: +39-011-0906999.
E-mail address: raffaella.sesana@polito.it

2452-3216
Peer-review under responsibility of the Scientific Committee of ICSI 2017
10.1016/j.prostr.2017.07.166

Keywords: Finite Element Method (FEM); additive manufacturing; stress analysis; Titanium alloy

1. Introduction

As is well known the so-called "Additive Manufacturing" (AM) includes several processes which allow shaping solids by a gradual addition of material, instead of some conventional machining operations which remove material [18]. Among the AM processes for metals, the powder bed deposition techniques are widely used. A layer of powder material is spread upon a platform built by either a roller or a blade. A hopper or a reservoir being located either below or aside the bed, provides the material supply. Material is consolidated by sintering/melting process by an energy supplier, as a laser or an electron beam. Layers are deposed and consolidated until that the whole three-dimensional object is created. The most popular powder bed processes are the Direct Metal Laser Sintering (DMLS), the Selective Laser Melting (SLM) and the Electron Beam Melting (EBM) [19].
Some materials are currently proposed for the AM, although the need of lightweight structures focused the attention of space engineering on the Titanium alloys [17] and particularly on the Ti-6Al-4V. The static strength of the AM Ti-6Al-4V was found comparable to that of wrought material, in terms of yield stress, ultimate strength and permanent elongation after rupture [8, 10, 12]. More difficult is a complete characterization of its performance in case of fatigue behavior [8, 11]. The surface roughness after the AM process usually makes worse the performance of material than in case of product made through some conventional process [8]. Nevertheless, mechanical and thermal treatments can significantly improve the fatigue life of the component [11]. It is known that the mechanical properties of AM product basically depend on some manufacturing parameters, powder quality, surface roughness and manufacturing irregularities, such as porosities and low density areas. Those are usually a consequence of a lower quality of raw powder or to an imperfect processing. A goal of current research activities is improving the process parameters and investigating the role of thermomechanical behavior in material deposition [15, 16].
The case study herein analyzed is a structural bracket for aerospace application, made of Ti-6Al-4V alloy through the AM techniques. The shape of bracket was defined by a topological optimization, aimed at reducing mass, limiting displacement and stress, and controlling the natural frequencies to satisfy some design requirements of the main system where the bracket will be assembled. It is worthy noticing that the optimization process reduced the mass of the original configuration to the 80% of its initial value. The shape was conformingly changed as shown in Fig.1. The new brackets were then produced by SLM and EBM.

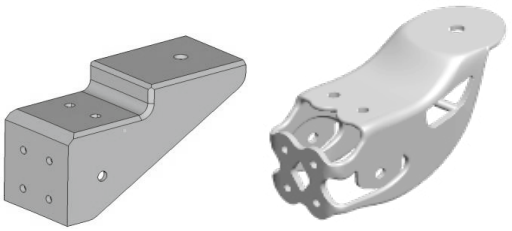

Fig. 1: Original (left) and optimized (right) shape of the analyzed bracket.

The research activity was aimed at assessing a design process to define the optimized shape of the bracket which could fit some customer needs. A key issue in modelling the mechanical component for design purpose concerns the material behavior. The presence of internal defects makes the material inhomogeneous, but inhomogeneities are randomly distributed within the volume of the mechanical component. A preliminary estimation of the mechanical behavior of material was therefore performed by assuming a homogeneous constitution of material, with average values of mechanical properties. This approach was already introduced in [7] and applied to lattice structures for bio-materials. It was demonstrated that the effect of material irregularities on the mechanical behavior can be taken into account when numerical models are developed, for instance, by defining a modified Young's modulus, to include the effect of porosity. This project belongs to the broader framework of the aerospace application, and its purpose basically was the understanding whether the AM process could enhance the performance and the production of this specific component. Other studies, such as [10], dealt with a straight evaluation of the mechanical behavior of AM-based components, without aiming at investigating the assessment of a product design procedure, thus mainly providing experimental evidence and testing of mechanical properties of the AM Titanium alloys, both at specimen and

component levels. Present work provides a validated procedure for a Finite Element Analysis (FEA) of the AM components, for design purpose. After that preliminary numerical activity performed through the FEM some experimental results are then reported, to describe the component behavior under static and fatigue loading.

2. Material characterization and modelling

A preliminary characterization of material Ti-6Al-4V obtained by AM was provided by an external supplier by resorting to static tests, namely the tensile test and the fracture test. Two lots of tensile test specimens were produced along different deposition directions, by using both the DMLS and EBM techniques. Up to 16 specimens were tested. They were obtained through a machining operation from raw cylinders, by fitting requirements of the ASTM E8 [1]. Results communicated are reported in Table 1, although they are related to a limited number of specimens.

Table 1: Tensile test results.

Material process		Yield (MPa) min÷max	UTS (MPa) min÷max	Elong. % min÷max
DMLS	X	1199÷1214	1322÷1339	7.0÷9.4
	Y	1201÷1217	1320÷1326	5.6÷8.0
EBM	X	1000÷1057	1077÷1127	13.2÷13.5
	Y	1007÷1107	1077÷1169	11.1÷13.7
	Z	973÷1029	1044÷1081	10.4÷11.2

For the DMLS specimens, some average values (standard deviation) were also provided. Set referred to as 'X' exhibited Yield = 1209 (7) MPa; UTS = 1329 (8) MPa; Elongation = 8.3 (1.0) %, while test referred to as 'Y' exhibited Yield = 1208 (6) MPa; UTS = 1323 (3) MPa; Elongation = 6.7 (0.9) %. In case of the EBM process, supplier did not provide average and standard deviation values.

Results of the fracture toughness test were successfully determined according to ASTM E399 [2]; three specimens were obtained by Electrical Discharge Machining (EDM) from larger blocks produced by EBM. Critical stress intensity factor (K_{IC}) was found equal to 60.3, 59.0 and 57.6 MPa$\sqrt{m}$, respectively for x, y and z samples.

Those values were used to define a simplified model of the elastic-plastic behavior of material to be inputted into the numerical model of the analyzed bracket.

3. Component numerical modeling

The complexity of bracket geometry required a numerical modelling activity to predict its behavior. The Finite Element Method was applied, by discretizing the system through several second-order tetrahedral elements. According to the space application foreseen, the loading conditions were simulated as Fig.3 shows. Particularly, at nodes where loads and constraints were applied (node 1 and nodes from 101 to 106) some RBE2 rigid elements were created. A large number of elements (up to 43160) and nodes (up to 78604) was used, to assure an accurate prediction of stress and strain, especially in correspondence of fillets and edges. An isotropic and homogeneous material model (MAT1) was assumed, with Young's modulus = 110000 MPa and Poisson's ratio = 0.34 according to the preliminary characterization of supplier. The FEM model was meshed and pre-processed by the Altair HyperMesh®13.0. All the degrees of freedom at nodes from 101 to 106 were constrained, while the external actions were applied to node 1. Three load cases were considered, as described in Fig.3. A linear static analysis (SOL 101) was performed by the FEM code MSC Nastran (Version 2014.0.0-CL305068).

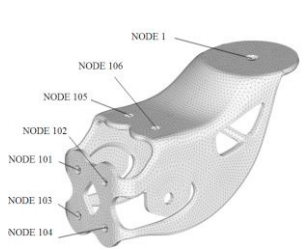

Fig. 2: Meshed geometry of bracket.

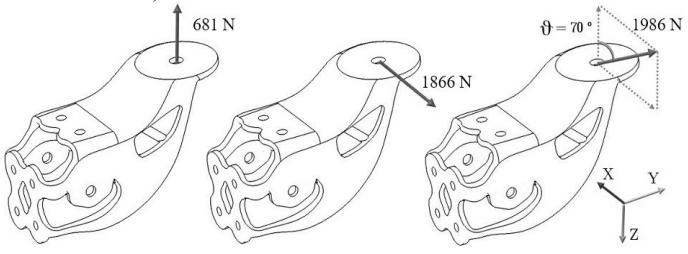

Fig. 3: Load cases 1 (left), 2 (middle) and 3 (right).

Under load case 1, the symmetry of component and the loading condition made the stress, displacement and reaction forces distributions symmetrical with respect of the middle longitudinal plane of the bracket, being identified by coordinates y,z. The maximum value of the equivalent Von Mises stress (296 MPa) was found at the edge below the plane identified by node 1, as shown in Fig. 4a. A fairly large stress values were also detected at the lower little arms near nodes 104 and 105, respectively. A maximum displacement of 0.5 mm was detected.
The load case 2 looks as an anti-symmetric loading condition, with respect of plane y,z, thus leading to a distribution of the equivalent Von Mises stress almost symmetric. Its maximum value (185 MPa) was found near constraints 105 and 106. Additional high stresses were detected at the rear arms, near 101 to 104 nodes. Those areas could be particularly critical, because of the small thickness and the likely presence of defects (see tomographic analysis of EBM brackets). The maximum displacement magnitude computed was 0.2 mm. It is worthy noticing that nodes 105 and 106 undergo a quite large axial loading (908 N) and even more shear action (4758 N)..
The load case 3 looks like a linear combination of load cases 1 and 2. Therefore, numerical results of the FEA show a superposition of stress induced by the two cases. A maximum equivalent Von Mises stress of 366 MPa was found where it was predicted in load case 1. The maximum displacement detected was 0.55 mm. Nodes 105 and 106 are the most critical ones because of the axial and shear actions applied. A maximum shear force of 5118 N was applied to node 106. As a preliminary evaluation of numerical results, the stresses occurring within the material of bracket do not reach a large magnitude, while actions on bolts applied to constrain the bracket looked fairly large. To validate the model, the distribution of strain for the load cases 1 and 3 were plotted in Figs.4 (d), (e) and (f).

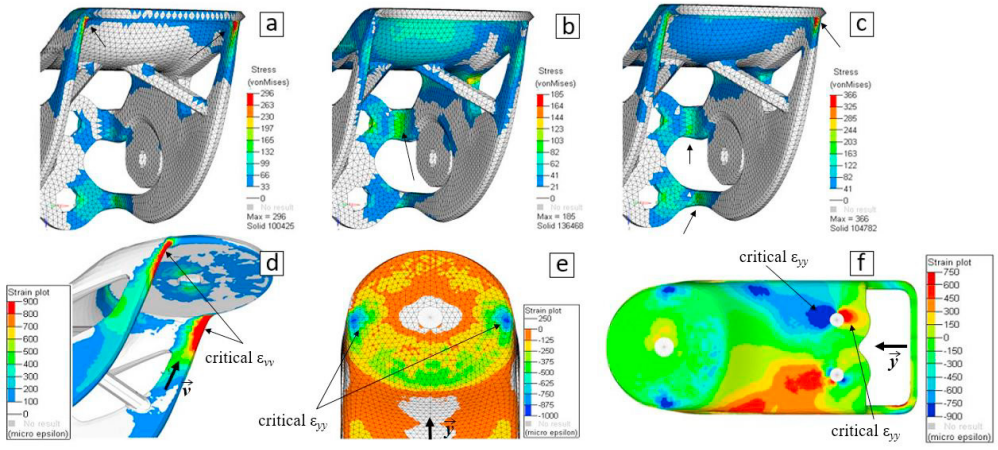

Fig. 4: FEM results: equivalent Von Mises stress distribution for load case 1 (a), 2 (b) and 3 (c); strain distributions for load case 1 (d),(e), and load case 3 (f).

4. Component testing

4.1. Test set-up

Several brackets were produced by AM in Ti-6Al-4V alloy to validate the models, both through the EBM and SLM processes. No heat treatment was applied to the EBM specimens, while heat treatment under Argon atmosphere was performed upon the SLM specimens. In addition, tumble finishing was executed on those brackets. In both cases, only the interface areas were machined. The detection of defects and the dimensional check were made through the X-ray and tomographic analysis. Monotonic tests were performed on the EBM brackets and two loading conditions were considered, as shown in Figs.5(a), (b) and (c). Configuration of constraints was replicating the actual constraining conditions of the real system, by considering the compliance of the main system interfaces. Therefore, brackets were connected through some M5 bolts to the lower platform of the test equipment, in correspondence to node 105 and 106, while M4 bolts were applied to nodes 101, 102, 103 and 104. To fit the project requirements, the grade of all bolts is 12.9. Like during a standard tensile test, the static strength of brackets was identified by applying an increasing load to reach in sequence three load levels called Limit Load (LL), Yield Load (YL) and Ultimate Load (UL), thus reaching

the condition for rupture. A reference ratio between those loads is defined by the required testing procedure. Particularly, the YL is 1.25 times the LL and the UL is twice the LL.
During the tests, transducers equipping the testing machine monitored and recorded the values of applied load and crosshead displacement. In each test, strain gauges were applied to measure the strain and to compare experimental and numerical results. They were located as Figs.5(d), (e) and (f) show, thus covering those areas which the FEA found critical for stress and strain (see Fig.4). It might be noticed that these brackets provide a specific function within the frame of a larger industrial system, being non disclosable. Basically it was required that no material yield occurs up to the application of the YL and no rupture occurs up to the UL application.

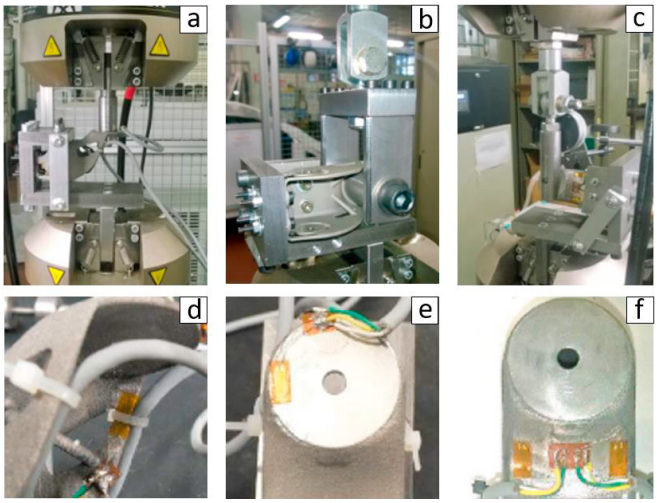

Fig. 5: First row: experimental set-up for the component static strength test: (a) load case 1; (b) load case 2; (c) load case 3. Second row: locations of the strain gauges for load case 1 (d), (e) and for load Case 2 and 3 (f).

Fatigue tests were also performed on both the EBM and SLM components. A sinusoidal load with a load ratio R=−1 with a maximum value equal to the Limit Load was applied, at 5 Hz. Two load cases were considered, according to the set-ups described in Fig.3, corresponding to case (a) and (b), respectively. For each value of load, one EBM and one SLM bracket were tested. It might be remarked that stress and displacements at the Limit Load are usually estimated by FEA, while the real fatigue life of the AM component is very difficult to be predicted, because of the complex geometry, high surface roughness and eventual presence of defects. However, a requirement for this space component was set at 150000 cycles of fatigue life.

4.2. Preliminary tomographic test of the components

As it was preliminarily remarked, an assessment of investigation tools for the design activity was required, to be compatible with the technological properties of this product as it looks after the AM process. Therefore, to proceed with static and fatigue tests on the built brackets, a preliminary detection of eventual defects lying on the surface or inside the material was performed to determine the real conditions for a validation of the numerical modelling activity proposed. A visual inspection was preliminarily performed on all of components. The SLM brackets showed a better surface finish compared to the EBM ones, as Fig. 6 shows.
To detect defects into the brackets the X-ray technique was applied. Nevertheless, the high roughness of surfaces did not allow reaching clear nor complete information. Therefore, the tomographic inspection was applied, thus classifying the material defects into Porosity and Low density areas. The first ones are more critical for the Failure Hazard Analysis (FHA) usually performed on the space system [20], while the second ones can be even non-hazardous defects. It is worthy noticing that few defects were detected within the SLM brackets (only one porosity in one bracket), while a large number of porosities and low-density areas were detected in the EBM products. Results were summarized in Table 2. Phi is the diameter of the smallest sphere including a defect. Some additional information could be found in 3D maps, as that depicted in Fig.6(e), to identify size, shape and location of defects.

Table 2: Results of tomographic defect detection on the EBM brackets tested.

Defect type	Number of defects avg (st.dev)	min Phi (mm)	max Phi (mm)	Defects vol. on total vol. % avg (st.dev)
Porosities	28.3 (8.7)	0.23	3.45	0.007 (0.003)
Low density areas	688 (48)	0.16	4.56	0.065 (0.013)

A dimensional check was performed through the tomographic analysis. Typical results are shown in Fig.6(f). Blue areas correspond to a lack of material in the real component; red color highlights areas where the real dimensions exceed the expected ones. In case of the SLM brackets, the comparison between geometric model and the real components highlighted a warping, while this effect did not appear in case of the EBM brackets.

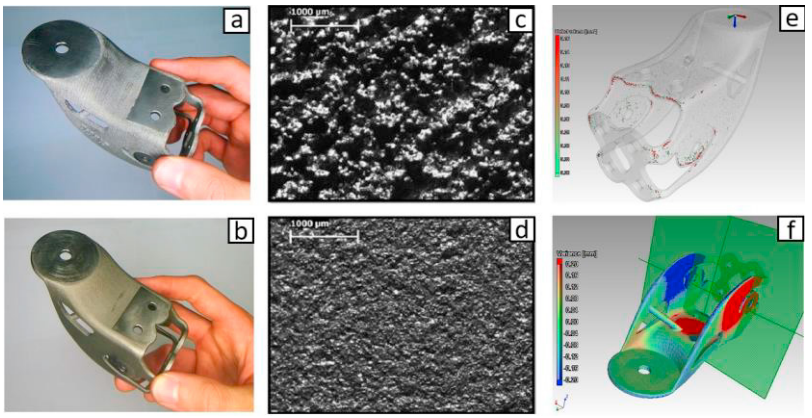

Fig. 6: Visual inspection on EBM (a) and SLM (b) products; high magnification of surface roughness for EBM (c) and SLM (d) brackets; results of defect detection through a tomographic exam performed on the EBM bracket (e); results of the dimensional check on the SLM bracket (f)

4.3. Static testing on components

Under the application of LL, YL and UL in load case 1, the brackets exhibited a linear elastic behavior, as Fig. 7a shows, in terms of relation between strain and applied load. Experimental measurements basically agree with FEA results, in terms of strain (400 με measured vs 450 με predicted) and displacement (0.20 mm measured vs 0.25 mm predicted). The rupture occurred in correspondence of node 1, where the bracket undergoes the effect of the external forces. Fracture occurred at 13500 N, therefore for a load fairly larger than the LL, in correspondence of a displacement equal to 11.2 mm. Similarly in load case 3, test showed a linear behavior with load. Strain values agreed with FEA results, for strain gage 1 (466 με measured vs 425 με predicted) and 2 (650 με measured vs 650 με predicted). Measured displacements were significantly higher. At the Limit load, the experimental displacement was about 1.25 mm, while FEM simulation predicted only 0.35 mm. This was related to a progressive failure of bolts, which introduced a rigid body motion in the measurement apparatus. Actually, when load was increased to reach the rupture, fasteners broke before than the bracket could reach the UL. A deformed M5 bolt is shown in Fig.7(c). The maximum load reached was slightly higher than 8500 N, and the maximum displacement was 24 mm.

4.4. Fatigue test

Concerning the load case 1, tests were stopped after 1 million cycles for both the EBM and SLM bracket, considering that the requirement was set at 150000 cycles. Nevertheless, no crack nor failure on the brackets were found. Applied load and displacements were recorded using the transducers equipping the test machine. That result suggested to the industrial partner to resort to some accelerated tests. Particularly, for the load case 2 the test plan was modified. After 500000 cycles, the maximum load was increased to the Yield Load (i.e. +25%). The first SLM bracket was tested and no crack was detected, even after 1 million of cycles. By converse, a rupture was found on the EBM bracket, after 729000 cycles. Fracture occurred in all of four arms near the fasteners. Fracture surface, described in Fig.7(d), shows multiple crack initiations, crack propagation and a final fracture surface on the left side. It must be noticed that fracture

occurs in those areas in which the tomography identified a widespread presence of porosity/low density areas.

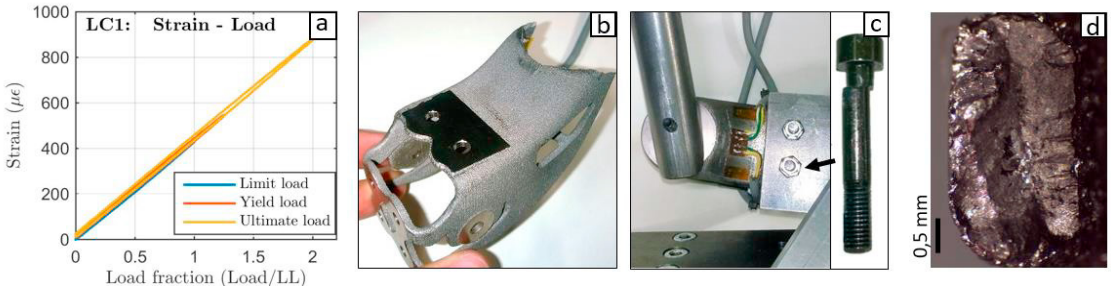

Fig. 7: Static tests - Load case 1 measured strain vs load fraction (a), Load case 1 failure (b), Load case 3 deformed fastener (c); Fatigue tests – Load case 2: detail of the fracture surface of the EBM bracket broken (d)

5. Discussion

Evaluating the mechanical performance of the structural bracket produced by AM for space application was a first goal of this investigation and the tests performed on the component demonstrated that strength is assured within the range of the mission requirements. However, investigating the limitations of some conventional approach to design in case of product based on AM process was even a target of this activity. It can be remarked that experiments performed on standard specimens show that the mechanical strength of the Ti-6Al-4V DMLS-alloy is similar to that of Ti-6Al-4V produced by conventional process, such as forging [5]. Moreover, those results agree with the data found in the specialized literature of AM [13]. Compared to the DMLS, the EBM structures exhibited a lower Yielding stress and UTS, and a larger elongation at rupture. Others studies already pointed out similar differences in mechanical properties between laser and electron beam technologies thus confirming this trend [14]. The fracture toughness, K_{Ic}, of the CT specimens tested in this study was close to values available in the literature [5] and consistent with values published in some handbook of wrought and annealed Ti-6Al-4V [6, 9].

Regarding the component testing activity, it is relevant that tomographic analysis found a large number of internal defects in the EBM components, while no defects were detected in the SLM products. This difference might be related to the thermal post processing performed on the SLM brackets. Moreover, a dimensional check pointed out some warping in SLM components, to be related to internal thermal stress generated by the large gradient of temperature associated to the process.

Static tests revealed that in both load cases 1 and 3, the component behavior seems to be linear up to the UL, thus confirming that no plasticity occurred up to twice the Limit Load (LL), as predicted by the FEM analysis. Despite of the large number of defects detected by the tomographic analysis, rupture occurred in both load cases at a much higher load. Test case 3 was affected by the rupture of fasteners, due to very high shear forces. This problem could suggest some change in the design of the whole system, although the bracket was verified.

Fatigue life in real operating condition looked different for the two processes. Test products exhibited a good fatigue behavior, especially in case of the SLM brackets, which did not reach the final rupture at least up to $1 \cdot 10^6$ cycles. Fracture occurred only in load case 2, on the EBM bracket, at 729000 cycles, although the requirement was fit (150000 cycles). A better fatigue behavior of the SLM brackets can be related to the lower number of internal defects and lower surface roughness. One must consider that on the SLM brackets was executed a heat treatment and tumble finishing, that could enhance the fatigue life. Further fatigue tests on standard specimens should be performed to evaluate the real fatigue performance of the Ti-6Al-4V produced by AM, but right now this activity was not yet allowed by the budget of this preliminary project. However, some research activities previously published [3, 4, 8, 11] showed that fatigue behavior of AM is almost equivalent to wrought material, when porosity is almost absent, the surface roughness immediately after the process is removed and the surface is thermally treated, at least for the processes which need to be, never the EBM [10].

The numerical modelling of the static behavior of AM Ti-6Al-4V components looked to be effective, in this case, for the specific geometry of bracket and the number of defects detected. Assumptions of homogeneous and isotropic material to define the constitutive laws of material were suitable in this case, but a preliminary investigation of defects is needed to define the limitations of this approach case by case.

6. Conclusion

This activity allowed the authors investigating how some design approaches, usually applied to metals and other materials, could be applied to the AM products. Three main peculiarities characterize this application, as the technical domain, i.e. the space engineering, the material, being the Titanium alloy Ti-6Al-4V, and the AM processes herein considered. It was possible realizing that design criteria are suitable, thanks to the tensile strength and the fracture toughness, being comparable to those of wrought Ti-6Al-4V. Nevertheless, the loading conditions of the analyzed product excite a lot the structure, therefore the two AM processes, namely the EBM and the SLM, exhibit a different performance in static and fatigue behaviors. This difference is basically related to the surface finish and the internal defects. Traditional tools like the tensile and fatigue tests and diagrams are still effective in this domain, if a preliminary detection of defects concentration is assured, for instance through a tomographic analysis of material. Macroscopic properties of material measured in tensile test can be used in numerical modelling up to a certain level of defects concentration. Fatigue life prediction might be affected by the distribution of internal defects, thus making this information crucial for an effective life prediction. Nevertheless, as a preliminary result the study identified a good strength of the proposed layout of bracket and some critical issues in bolted joints. It provided to the industrial partner a suitable procedure to verify and validate the product development of the AM based components.

References

[1] ASTM Standard E8 "Standard test method for tension testing of metallic materials (Metric)." American Society for Testing and Materials, Philadelphia, PA (1993).
[2] ASTM Standard E399-90, "Standard test method for plane strain fracture toughness of metallic materials." American Society for Testing and Materials, Philadelphia, PA (1993).
[3] Baufeld, B., Brandl, E., and Biest, O., 2011, “Wire Based Additive Layer Manufacturing: Comparison of Microstructural and Mechanical Properties of Ti-6Al-4V Components Fabricated by Laser-Beam Deposition and Shaped Metal Deposition” J. Mater. Process. Technol., 211, pp.1146–1158.
[4] Brandl, E., Baufeld, B., Leynes, C., and Gault, R., 2010, “Additive Manufactured Ti-6Al-4V Using Welding Wire: Comparisons of Laser and Arc Beam Deposition and Evaluation With Respect to Aerospace Material Specifications,” Phys. Procedia, 5, pp.595–606.
[5] Brecht Van Hooreweder et al., 2012, “Analysis of fracture toughness and crack propagation of Ti6Al4V produced by selective laser melting”, Advanced Engineering Materials 14.1-2, pp.92–97.
[6] Cameron, D. W., and Hoeppner, D. W., 1996, “Fatigue Properties in Engineering”, ASM Handbook: Fatigue and Fracture, ASM International, Materials Park, OH, Vol. 19, p.15.
[7] Campoli, G., et al., 2013, "Mechanical properties of open-cell metallic biomaterials manufactured using additive manufacturing." Materials & Design 49, pp.957-965.
[8] Chan, K., Koike, M., Mason, R., and Okabe, T., 2013, “Fatigue Life of Titanium Alloys Fabricated by Additive Manufacturing Techniques for Dental Implants,” Metall. Mater. Trans. A, 44A, pp.1010–1022.
[9] Collings, E. W., Materials Properties Handbook: Titanium Alloys, ASTM International, Materials Park, OH 1994.
[10] Edwards, P., O'Conner, A., and Ramulu., M., 2013, "Electron beam additive manufacturing of titanium components: properties and performance." Journal of Manufacturing Science and Engineering 135.6.
[11] Facchini, L., Magalini, E., Robotti, P., and Molinari, A., 2009, “Microstructure and Mechanical Properties of Ti-6Al-4V Produced by Electron Beam Melting of Pre-Alloyed Powders,” Rapid Prototyping J., 15(3), pp.171–178.
[12] Koike, M., et al., 2011, "Evaluation of titanium alloys fabricated using rapid prototyping technologies—electron beam melting and laser beam melting." Materials 4.10, pp.1776-1792.
[13] Leuders, S., Thone, M., Riemer, A., Niendorf, T., Troster, T., Richard, H., and Maier, J., 2013, “On the Mechanical Behavior of Titanium Alloy Tial6v4 Manufacture by Selective Laser Melting: Fatigue Resistance and Crack Growth Performance,” Int. J. Fatigue, 48, pp.300–307.
[14] Murr, L. E., et al., 2009, "Microstructure and mechanical behavior of Ti–6Al–4V produced by rapid-layer manufacturing, for biomedical applications." Journal of the mechanical behavior of biomedical materials 2.1, pp.20-32.
[15] Romano, J., Ladani, L., Sadowski, M., 2015, "Thermal modeling of laser based additive manufacturing processes within common materials." Procedia Manufacturing 1, pp.238-250.
[16] Yang, Q., et al., 2016, "Finite element modeling and validation of thermomechanical behavior of Ti-6Al-4V in directed energy deposition additive manufacturing." Additive Manufacturing 12, pp.169-177.
[17] Dutta, B., Froes, F., Additive manufacturing of Titanium alloys: state of the art, challenges and opportunities, Springer, 2016.
[18] Gibson, I., Rosen, D., Stucker, B., Additive manufacturing technologies: 3D printing, rapid prototyping and direct digital manufacturing, Springer, 2016.
[19] Gu, D., Laser additive manufacturing of high-performance materials, Springer, 2016.
[20] Stigliani, C., Ferretto, D., Pessa, C., Brusa, E., “A model based approach to design for reliability and safety of critical aeronautic systems”, Proc. INCOSE Conf. on Systems Engineering (CIISE 2016), Turin, Italy, November 14-15, 2016, CEUR-WS.org/Vol.1728; urn:nbn:de:0074-1728-8, pp.56–64.